



**HAL**  
open science

## Sensitivity Analysis Using the Virtual Work Principle For 2D Magnetostatic Problems

Olivier Brun, Olivier Chadebec, Pauline Ferrouillat, Innocent Niyonzima,  
Jonathan Siau, Gérard Meunier, Laurent Gerbaud, Frédéric Vi, Yann Le Floch

► **To cite this version:**

Olivier Brun, Olivier Chadebec, Pauline Ferrouillat, Innocent Niyonzima, Jonathan Siau, et al.. Sensitivity Analysis Using the Virtual Work Principle For 2D Magnetostatic Problems. IEEE Transactions on Magnetics, 2023, 59 (5), 10.1109/TMAG.2023.3237030 . hal-03892407

**HAL Id: hal-03892407**

**<https://hal.science/hal-03892407v1>**

Submitted on 9 Dec 2022

**HAL** is a multi-disciplinary open access archive for the deposit and dissemination of scientific research documents, whether they are published or not. The documents may come from teaching and research institutions in France or abroad, or from public or private research centers.

L'archive ouverte pluridisciplinaire **HAL**, est destinée au dépôt et à la diffusion de documents scientifiques de niveau recherche, publiés ou non, émanant des établissements d'enseignement et de recherche français ou étrangers, des laboratoires publics ou privés.

# Sensitivity Analysis Using the Virtual Work Principle For 2D Magnetostatic Problems

Olivier Brun<sup>1,2</sup>, Olivier Chadebec<sup>1</sup>, Pauline Ferrouillat<sup>2</sup>, Innocent Niyonzima<sup>1</sup>, Jonathan Siau<sup>2</sup>, Gérard Meunier<sup>1</sup>, Laurent Gerbaud<sup>1</sup>, Frédéric Vi<sup>2</sup> and Yann Le Floch<sup>2</sup>

<sup>1</sup>Univ. Grenoble Alpes, CNRS, Grenoble INP, G2ELab, Grenoble, France

<sup>2</sup>Altair Engineering, Meylan, France

The sensitivity analysis of electromagnetic quantities such as the magnetic force and torque is a crucial step when optimizing electromagnetic devices with gradient-based optimizers. This paper provides an analytical derivation of those two quantities using the virtual work principle in a finite element package. It is suitable for any kind of optimization. A focus on the particular use of this sensitivity on shape optimization is presented. The development and validation of the method is detailed in this case. Finally, it is applied to the shape optimization of a switch reluctance motor (SRM) to improve its performances.

*Index Terms*—Sensitivity analysis, Virtual work method, Shape optimization, Electrical machine design.

## I. INTRODUCTION

THE optimization of electromagnetic devices is a popular topic. It allows to improve existing devices or to find new ones which may not be intuitive. Three types of optimization can be distinguished: parametric, shape and topology optimization. The main difference between those setups is the nature of the design space. In a parametric context, one mainly aims at optimizing predefined parameters [1], for instance geometric parameters. For shape optimization, it is the border nodes of an initial design which are considered [1], [2]. In the case of topology optimization, the goal is to distribute a given amount of ferromagnetic material in the mesh elements of a chosen optimization region. The SIMP method [1] or the Level-set method [3] can be used.

Regardless of the optimization type, genetic algorithms can be numerically used. They converge towards the global optimum but are known to use unreasonable computation time when the number of optimization parameters becomes large. Another choice is the use of gradient-based algorithms. They converge faster but might be stuck in local optimums. A crucial step when using those algorithms is a precise computation of the sensitivity with respect to the design variables of the optimization. A basic finite difference method can be used, which is easy to implement but numerically slow and unstable. A widely used alternative is an analytical derivation of the optimization objective, coupled with the adjoint method in order to keep an acceptable computation time. The adjoint method is presented in many papers, for instance in [1], [2] and [3].

A classical optimization for electromagnetic devices such as actuators or motors is to maximize the magnetic force or torque in their mobile part while constraining the volume of the device and possibly other electromagnetic quantities.

In [4] and [5], the Maxwell tensor method is used to compute the force and its sensitivity using the adjoint method.

The virtual work method [6] is another method to compute the force as the derivative of the magnetic energy. It is known to have a better accuracy [7]. Another advantage compared to the Maxwell tensor is that it does not require the additional choice of a path surrounding the region where the force is computed.

In [8], the adjoint method was used on a virtual work formulation, but it uses the finite difference method. This paper provides a fully analytical sensitivity analysis of the magnetic force and torque via the virtual work method using the adjoint method. To our knowledge, this has never been done before.

Section II presents the magnetostatic context of the study, and the state of the art of the sensitivity analysis using the adjoint method. Section III presents the specific application of the adjoint method to the magnetic force and torque sensitivity computed using the virtual work method in a general optimization setup. Section IV details the specific application of section III to shape optimization and finally section V shows an example of its use on the optimization of a SRM built with a nonlinear ferromagnetic material.

## II. STATE OF THE ART

### A. Magnetostatic context

Let  $\Omega$  be the 2D domain of study. A current supply is represented using a density  $\mathbf{J} = J_z \mathbf{e}_z$  in a region  $\Omega_S$  and zero elsewhere. Let  $\Omega_F$  be a domain filled with a ferromagnetic material, possibly with nonlinear characteristics. The current  $\mathbf{J}$  creates a magnetic force or torque on  $\Omega_F$ .

The magnetostatic equations with 2D assumptions satisfied in  $\Omega$  are :

$$\begin{aligned} \nabla \times \mathbf{H} &= 0 \quad \text{in } \Omega \setminus \Omega_S, \\ \nabla \times \mathbf{H} &= \mathbf{J} \quad \text{in } \Omega_S, \\ \mathbf{H} &= \nu \mathbf{B} ; \mathbf{B} = \nabla \times \mathbf{A}_z, \\ \mathbf{A}_z &= 0 \quad \text{on } \partial\Omega, \end{aligned} \quad (1)$$

where  $\mathbf{H}$  is the magnetic field ( $A.m^{-1}$ ),  $\mathbf{B}$  is the magnetic induction ( $T$ ),  $\mathbf{A}_z = A_z \mathbf{e}_z$  is the 2D potential vector and

$\nu$  is the magnetic reluctivity. In the air regions, one has  $\nu = \nu_0$  with  $\nu_0$  the vacuum reluctivity. In the regions filled with ferromagnetic materials, including  $\Omega_F$ ,  $\nu$  is described by nonlinear laws  $\nu = \nu(|\mathbf{B}|)$ .

This nonlinear scalar equation (1) is solved using the Newton-Raphson algorithm which iteratively solves the following matrix system :

$$S(\mathbf{A}^{(k-1)})\mathbf{A}^{(k)} = \mathbf{b}^{(k-1)} \quad (2)$$

where  $\mathbf{A}^{(k)}$  is the vector of values of the potential vector  $\mathbf{A}_z$  discretized on the mesh nodes of the domain  $\Omega$  at the  $k^{\text{th}}$  current iteration of the Newton-Raphson algorithm.

### B. The adjoint method

Let  $F$  be a scalar function of interest that has to be optimized and  $(X_i)_{1 \leq i \leq n}$  some design variables in a general optimization context.  $\bar{F}$  is a function of the design variables and of the state variable:  $F = F(\mathbf{A}, X_1, \dots, X_n)$  with  $\mathbf{A} = (A_j)_{j=1, \dots, m}$  the nodal values of the vector potential. Assuming that the Newton-Raphson algorithm (2) converges in  $K+1$  iterations, the state variable  $\mathbf{A}$  is obtained by solving a linear system  $S^{(K)}\mathbf{A} = \mathbf{b}^{(K)}$ . The sensitivity using the adjoint method reads [1]:

$$\frac{dF}{dX_i} = \frac{\partial F}{\partial X_i} + \boldsymbol{\lambda}^T \left( \frac{d\mathbf{b}^{(K)}}{dX_i} - \frac{dS^{(K)}}{dX_i} \mathbf{A} \right). \quad (3)$$

with  $\boldsymbol{\lambda}$  the adjoint vector defined as the solution of :

$$S^{(K)}\boldsymbol{\lambda} = \frac{\partial F}{\partial \mathbf{A}}. \quad (4)$$

The strength of this method is that  $\boldsymbol{\lambda}$  is the solution of a linear matrix system already built during the physical solving (2). The terms  $\frac{d\mathbf{b}^{(K)}}{dX_i}$  and  $\frac{dS^{(K)}}{dX_i}$  can be analytically expressed from the finite element assembly.

## III. SENSITIVITY ANALYSIS WITH THE VIRTUAL WORK METHOD

### A. The virtual work method for magnetic force and torque

The virtual work method allows to compute the magnetic force on  $\Omega_F$  as the derivative of the magnetic energy  $W = \int_{\Omega} \int_0^B H(b)db d\Omega$  along a direction  $s$  at constant state variable  $\mathbf{A}$ . After breaking down the integral over the mesh, its expression is [6]:

$$F_s = -\frac{\partial W}{\partial s} = \nu_0 \sum_e \int_{\Omega_e} \mathbf{B}^T M_e \mathbf{B} \, d\Omega \quad (5)$$

$$\text{with } M_e = -G_e^{-1} \frac{\partial G_e}{\partial s} + \frac{1}{2|G_e|} \frac{\partial |G_e|}{\partial s} I,$$

where  $G_e$  is the Jacobian matrix of the transformation from the mesh element  $\Omega_e$  to the reference element  $\Delta_e$  [6],  $|G_e|$  its determinant and  $I$  is the identity matrix.

The terms  $\frac{\partial G_e}{\partial s}$  and  $\frac{\partial |G_e|}{\partial s}$  are the derivatives of  $G_e$  and  $|G_e|$  with respect to the translation of the mesh nodes of  $\Omega_F$  in the direction  $s$ . They are zero everywhere except in the first air layer of mesh elements surrounding  $\Omega_F$ .

The same formula remains true for the torque around an axis  $\omega$ , but in this case the mesh nodes of  $\Omega_F$  are moved with a rotating movement around  $\omega$ .

### B. Expression of the sensitivity

As the adjoint vector  $\boldsymbol{\lambda}$  is the solution of the linear problem (4), the term  $\frac{\partial F_s}{\partial \mathbf{A}}$  has to be expressed in the case of the force (5). One has:

$$\frac{\partial F_s}{\partial \mathbf{A}} = \left( \frac{\partial F_s}{\partial \mathbf{B}} \right)^T \frac{\partial \mathbf{B}}{\partial \mathbf{A}}. \quad (6)$$

Since  $\mathbf{B} = \sum_{j=1}^m A_j \nabla \times \boldsymbol{\tau}_j$  with  $\boldsymbol{\tau}_j$  the 2D nodal shape function at node  $j$ , the vector  $\frac{\partial \mathbf{B}}{\partial \mathbf{A}}$  can be immediately written as :

$$\left( \frac{\partial \mathbf{B}}{\partial \mathbf{A}} \right)_{1 \leq j \leq m} = (\nabla \times \boldsymbol{\tau}_j)_{1 \leq j \leq m}. \quad (7)$$

The magnetic force has an explicit formula in term of  $\mathbf{B}$  field (5) that can be directly differentiated.

$$\frac{\partial F_s}{\partial \mathbf{B}} = \nu_0 \sum_e \int_{\Omega_e} (M_e + M_e^T) \mathbf{B} d\Omega \quad (8)$$

Combining the two last equations, it is possible to build  $\frac{\partial F_s}{\partial \mathbf{A}}$  and to solve the adjoint equation (4). The adjoint state is the same regardless of the chosen type of optimization. Then, the sensitivity can be computed using (3).

However, the term  $\frac{\partial F_s}{\partial X_i}$  in (3) depends on the considered optimization type. Since the support of the magnetic force is the first air mesh layer surrounding  $\Omega_F$ ,  $\frac{\partial F_s}{\partial X_i}$  is non zero only when the parameters  $(X_i)_{1 \leq i \leq n}$  influence the mesh elements of this layer. For instance, when the SIMP method is used in the case of topology optimization,  $\frac{\partial F_s}{\partial X_i}$  is always zero. The next section details the case of shape optimization, where  $\frac{\partial F_s}{\partial X_i}$  can be non-zero.

## IV. SPECIFIC CASE OF SHAPE OPTIMIZATION

### A. Explicit dependency of the force on the design variables

In the case of shape optimization, the design variables are the nodes  $(X_i)_{1 \leq i \leq n}$  of the border lines of an initial design. The adjoint state can be solved using (4) and (6). The term  $\frac{\partial F_s}{\partial X_i}$  in (3) is zero in general except when optimizing the border lines of  $\Omega_F$ . In this case, the optimization is performed at the same place where the force is computed. It means that there is an explicit dependency of the force on the  $X_i$  variables and the term  $\frac{\partial F_s}{\partial X_i}$  is non-zero. It must be taken into account but its development and implementation is tedious.

The term has been expressed by applying twice the virtual work principle on the magnetic energy  $W$ , which leads to :

$$\begin{aligned} \frac{\partial F_s}{\partial X_i} = -\frac{\partial^2 W}{\partial s \partial X_i} = & \sum_{e=1}^N \int_{\Delta_e} \left( \frac{\partial^2 |G_e|}{\partial s \partial X_i} \int_0^H \mathbf{B} d\mathbf{H} \right. \\ & - \mathbf{B}^T \mathbf{H} \frac{\partial |G_e|}{\partial s} \frac{\partial |G_e|}{\partial X_i} \frac{1}{|G_e|} \\ & + \mathbf{B}^T \frac{\partial G_e}{\partial X_i} G_e^{-T} \mathbf{H} \frac{\partial |G_e|}{\partial s} \\ & + \mathbf{B}^T G_e^{-1} \frac{\partial G_e}{\partial s} \mathbf{H} \frac{\partial |G_e|}{\partial X_i} \\ & - \mathbf{B}^T G_e^{-1} \frac{\partial^2 G_e}{\partial s \partial X_i} \mathbf{H} |G_e| \\ & \left. - \mathbf{B}^T G_e^{-1} \frac{\partial G_e}{\partial s} \frac{\partial G_e}{\partial X_i} G_e^{-T} \mathbf{H} |G_e| \right) d\Delta_e, \end{aligned} \quad (9)$$

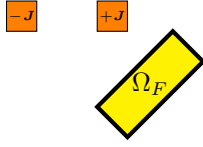


Fig. 1: Geometry of the academic test case

where the terms  $\frac{\partial G_e}{\partial X_i}$ ,  $\frac{\partial |G_e|}{\partial X_i}$ ,  $\frac{\partial^2 G_e}{\partial s \partial X_i}$  and  $\frac{\partial^2 |G_e|}{\partial s \partial X_i}$  are respectively the derivatives of the previous terms  $G_e$ ,  $|G_e|$ ,  $\frac{\partial G_e}{\partial s}$  and  $\frac{\partial |G_e|}{\partial s}$  with respect to the virtual translation of the node  $X_i$  in the direction of computation of the sensitivity. They are zero everywhere except on the elements that contain  $X_i$ . This formula is deduced using the specificity of the potential vector formulation. Indeed, the transformation to the reference space requires the use of a Piola transform which is not the same for scalar and vector formulations [9]. Using a scalar potential formulation  $\mathbf{H} = -\nabla\psi$  would lead to a different formula. See [6] for a detailed use of the scalar formulation on the virtual work method.

### B. Validation

The sensitivity (3) of the magnetic force and torque has been implemented in the case of shape optimization, including (6) and the tedious term (9). A validation step has been performed on a simple bidimensional academic test case using the following (central) finite difference method to confirm the implementation :

$$\frac{dF_s}{dX_i} \approx \frac{F_s(X_i + \epsilon) - F_s(X_i - \epsilon)}{2\epsilon}. \quad (10)$$

In the context of shape optimization,  $X_i + \epsilon$  stands for a slight disturbance of the coordinates of  $X_i$  either in the horizontal or the vertical direction, depending on the direction of computation of the sensitivity.

The geometry of the test case is presented in Figure 1. A current supply is represented by the orange coil. A region  $\Omega_F$  is filled with a nonlinear ferromagnetic material. The sensitivities of the force and torque on  $\Omega_F$  are calculated on the  $n = 77$  mesh nodes of  $\Omega_F$  (thick lines on figure 1).

The finite difference method is really slow since it requires  $2n$  nonlinear finite element solvings per sensitivity computation direction. Figures 2 and 3 compare the sensitivity values obtained analytically and with finite differences. The results are close to each other. The maximum relative error between the two methods is lower than 1%.

## V. APPLICATION

### A. Optimization workflow

After the concluding validation step, the sensitivity code has been included in a gradient-based shape optimization workflow using the softwares Altair Flux<sup>TM</sup> and Optistruct<sup>TM</sup>. Starting from a given design, the sensitivity is used to update the current optimization nodes in a descent direction. Then, the process iterates until the optimization converges to an optimal design or a maximum number of iteration is reached.

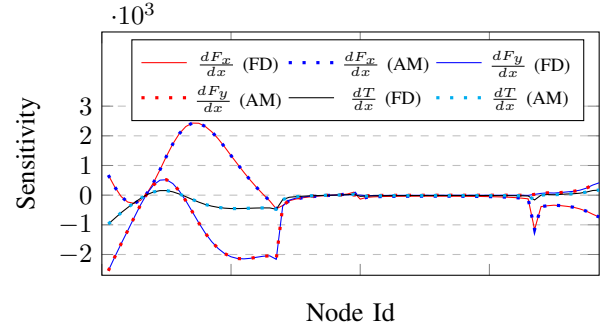


Fig. 2: Sensitivity with respect to an horizontal displacement of the nodes obtained with the finite difference method (FD) and the adjoint method (AM)

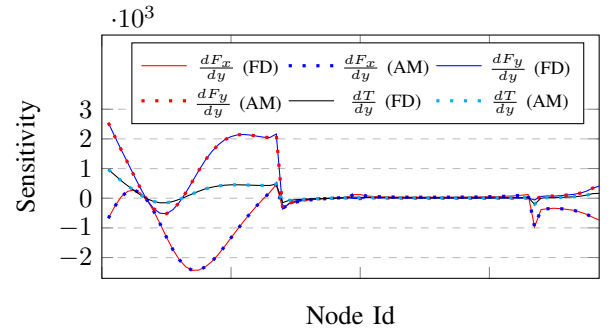


Fig. 3: Sensitivity with respect to a vertical displacement of the nodes obtained with the finite difference method (FD) and the adjoint method (AM)

### B. Optimization problem

This optimization algorithm is applied on a realistic SRM model presented in figure 4. The stator (in orange) and rotor (in grey) are made of a laminated nonlinear ferromagnetic material. The current supply in the stator has three winding phases represented in red, blue, green and brown. Thanks to the geometrical and electrical symetries, only one quarter of the motor can be represented. The light blue color represents the air regions of the device.

The torque depends on the position of the rotor. Thus, the angular position of the rotor is discretized in  $N = 30$  positions  $(\theta_i)_{1 \leq i \leq N}$  to compute it in every rotor configuration.

The main objective is to maximize the mean torque value  $T_{mean}$  over all the rotor positions :

$$T_{mean} = \frac{1}{N} \sum_{i=1}^N T(\theta_i), \quad (11)$$

with  $T(\theta_i)$  the torque computed at the angular position  $\theta_i$ .

The SRM are known to have a large torque amplitude over a rotation. This leads to noisy motors. A relative measure of this amplitude is given by the torque ripple  $T_r$  :

$$T_r = 100 \times \frac{T_{max} - T_{min}}{T_{mean}}, \quad (12)$$

where  $T_{min} = \min_{1 \leq i \leq N} T(\theta_i)$  and  $T_{max} = \max_{1 \leq i \leq N} T(\theta_i)$ .

The torque ripple must remain under an acceptable value  $T_r^{max}$  in the optimized design. The sensitivity of the

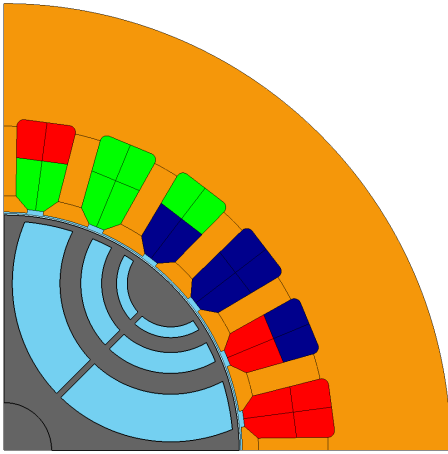


Fig. 4: View of the initial SRM rotor design

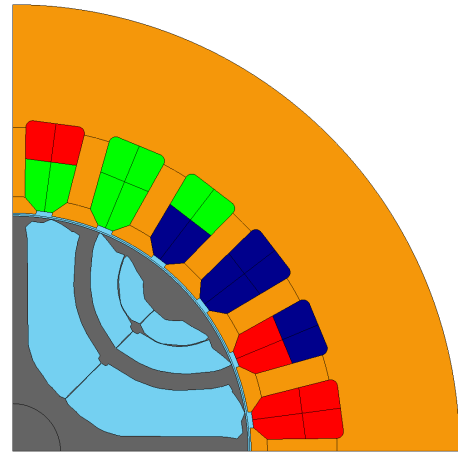


Fig. 5: View of the optimized SRM rotor design

mean torque and torque ripple are easily computed since they are basic functions of the  $T(\theta_i)$  values.

A constraint on the rotor volume  $V$  is also enforced to reduce by 20% the initial volume  $V_0$  of the rotor represented in figure 4 and avoid the use of the expensive ferromagnetic material. The design variables of the shape optimization are the nodes  $(X_i)_{1 \leq i \leq 886}$  of the lines inside the rotor in contact with the air regions. The final optimization problem is the following :

$$\begin{aligned} & \underset{X_i}{\text{maximize}} && T_{mean}(X_i) \\ & \text{subject to} && T_r(X_i) \leq T_r^{max}, \\ & && V \leq 0.8 \times V_0 \end{aligned} \quad (13)$$

### C. Results

After thirty optimization iterations and about two hours of computation, the optimized design shown in figure 5 has been obtained. The final design has a mean torque 38% higher than the initial one, while the mass of its rotor has decreased by 20% and its torque ripple decreased by 31%. Figure 6 shows the torque as a function of the angular position of the rotor for the initial and final designs. The optimized electrotechnical features are really interesting, however the final design clearly lacks of mechanical strength to be used in a real application for now.

## VI. CONCLUSION

The sensitivity analysis of the magnetic force and torque is analytically derived using the virtual work method. The expression of the sensitivity relies on the well known adjoint method, but it had never been applied to the virtual work method before. The sensitivity expression is presented in a general optimization context. Then, it is applied to the specific case of shape optimization. Finally, the use of this sensitivity analysis on the shape optimization of a SRM shows an interesting final design with an improved torque and reduced volume and torque ripple. An application of this method in the 3D case could be studied with a cautious adaptation of the explicit dependency (9) depending on the formulation (vector or scalar) which is used.

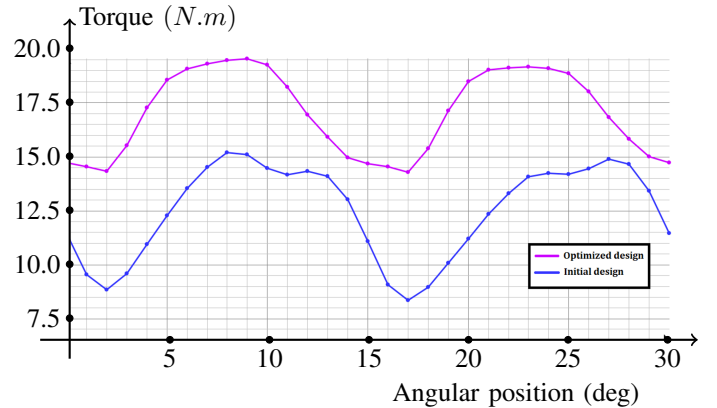


Fig. 6: Comparison of torque value as a function of the angular rotor position before and after the optimization

## REFERENCES

- [1] Zhou, M., Pagaldipti, N., Thomas, H. L., & Shyy, Y. K. (2004). An integrated approach to topology, sizing, and shape optimization. *Structural and Multidisciplinary Optimization*, 26(5), 308-317.
- [2] Kim, D. H., Ship, K. S., & Sykulski, J. K. (2004). Applying continuum design sensitivity analysis combined with standard EM software to shape optimization in magnetostatic problems. *IEEE Transactions on Magnetics*, 40(2), 1156-1159.
- [3] Kim, D-H., Jan K. Sykulski, & David A. Lowther (2007). "Design optimisation of electromagnetic devices using continuum design sensitivity analysis combined with commercial EM software." *IET Science, Measurement & Technology* 1.1 : 30-36.
- [4] Labbe, T., & Dehez, B. (2011). Topology optimization method based on the Maxwell stress tensor for the design of ferromagnetic parts in electromagnetic actuators. *IEEE transactions on magnetics*, 47(9).
- [5] Lee, S. W., Lee, J., & Cho, S. (2015). Isogeometric shape optimization of ferromagnetic materials in magnetic actuators. *IEEE Transactions on Magnetics*, 52(2), 1-8.
- [6] Coulomb, J. (1983). A methodology for the determination of global electromechanical quantities from a finite element analysis and its application to the evaluation of magnetic forces, torques and stiffness. *IEEE Transactions on Magnetics*, 19(6), 2514-2519.
- [7] Ren, Z. (1994). Comparison of different force calculation methods in 3D finite element modelling. *IEEE Transactions on Magnetics*, 30(5).
- [8] Yoo, J., Yang, S., & Choi, J. S. (2008). Optimal design of an electromagnetic coupler to maximize force to a specific direction. *IEEE Transactions on Magnetics*, 44(7), 1737-1742.
- [9] Zaglmayr, S. (2006). High Order Finite Element Methods for Electromagnetic Field Computation. PhD thesis.